

## **Electronic Supplementary Information**

### **Hierarchical Structure in Poly(*N*-vinyl carbazole)/Fe<sub>3</sub>O<sub>4</sub> Nanocomposites and the Relevant Magnetic Coercivity**

Meng Z. Chen,<sup>a</sup> Che Y. Chu,<sup>\*a</sup> Bradley W. Mansel<sup>b</sup> and Po C. Chang<sup>a</sup>

<sup>a</sup> Department of Chemical Engineering, National Chung Hsing University, Taichung 402, Taiwan

E-mail: [cychu0123@dragon.nchu.edu.tw](mailto:cychu0123@dragon.nchu.edu.tw)

<sup>b</sup> Institute of Fundamental Sciences, Massey University, Palmerston North 4474, New Zealand

The Electronic Supplementary Information contains the following figures.

1. FTIR spectra of PVP-Fe<sub>3</sub>O<sub>4</sub> nanoparticles, acrylic acid and AA-Fe<sub>3</sub>O<sub>4</sub> nanoparticles (**Figure S1**)
2. TGA curve of AA-Fe<sub>3</sub>O<sub>4</sub> nanoparticles (**Figure S2**)
3. TGA curves of PNVK/AA-Fe<sub>3</sub>O<sub>4</sub> nanocomposites (**Figure S3**)
4. Flowchart of nanoparticle cluster building code (**Figure S4**)
5. GPC curves of neat PNVK samples polymerized at different polymerization protocols (**Figure S5**)
6. SAXS profile of Fe<sub>3</sub>O<sub>4</sub> nanoparticles dissolved in DMF solvent (**Figure S6**)
7. Hysteresis loop of neat PNVK polymer (**Figure S7**)

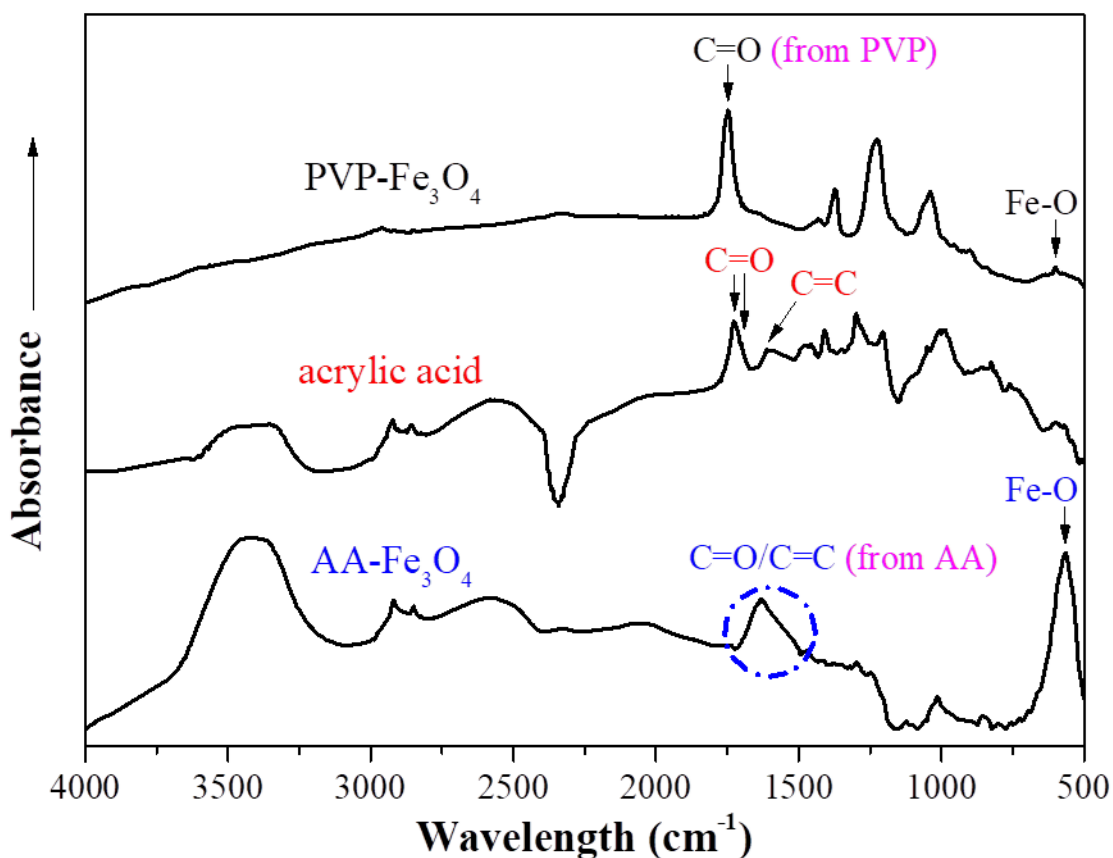


**Figure S1.** FTIR spectra of the PVP-Fe<sub>3</sub>O<sub>4</sub> nanoparticles, acrylic acid, and AA-Fe<sub>3</sub>O<sub>4</sub> nanoparticles. The signals of bands from the Fe-O stretching and the C=O functional group in PVP-Fe<sub>3</sub>O<sub>4</sub> nanoparticles were found at 600 and 1747 cm<sup>-1</sup>, respectively, while those from the C=C and C=O functional groups in acrylic acid were observed at 1613 and 1700 cm<sup>-1</sup>, respectively. For the AA-Fe<sub>3</sub>O<sub>4</sub> nanoparticles, the appearance of an overlapped broad peak at 1635 cm<sup>-1</sup> (attributed to the signals of bands from both the C=C and C=O functional groups in acrylic acid)<sup>35-37</sup> and a peak at 565 cm<sup>-1</sup> (attributed to the signal of the band from the Fe-O stretching in Fe<sub>3</sub>O<sub>4</sub>)<sup>38</sup> denoted that the Fe<sub>3</sub>O<sub>4</sub> nanoparticles have been successfully modified by acrylic acid. On the other hand, the appearance of the broad peak around 3400 cm<sup>-1</sup> for both the acrylic acid and

AA-Fe<sub>3</sub>O<sub>4</sub> nanoparticles was attributed to the O-H stretching band of absorbed water molecules, which consisted of a symmetric stretching absorption at 3220 cm<sup>-1</sup> and an antisymmetric stretching absorption at 3445 cm<sup>-1</sup>.<sup>39,40</sup>

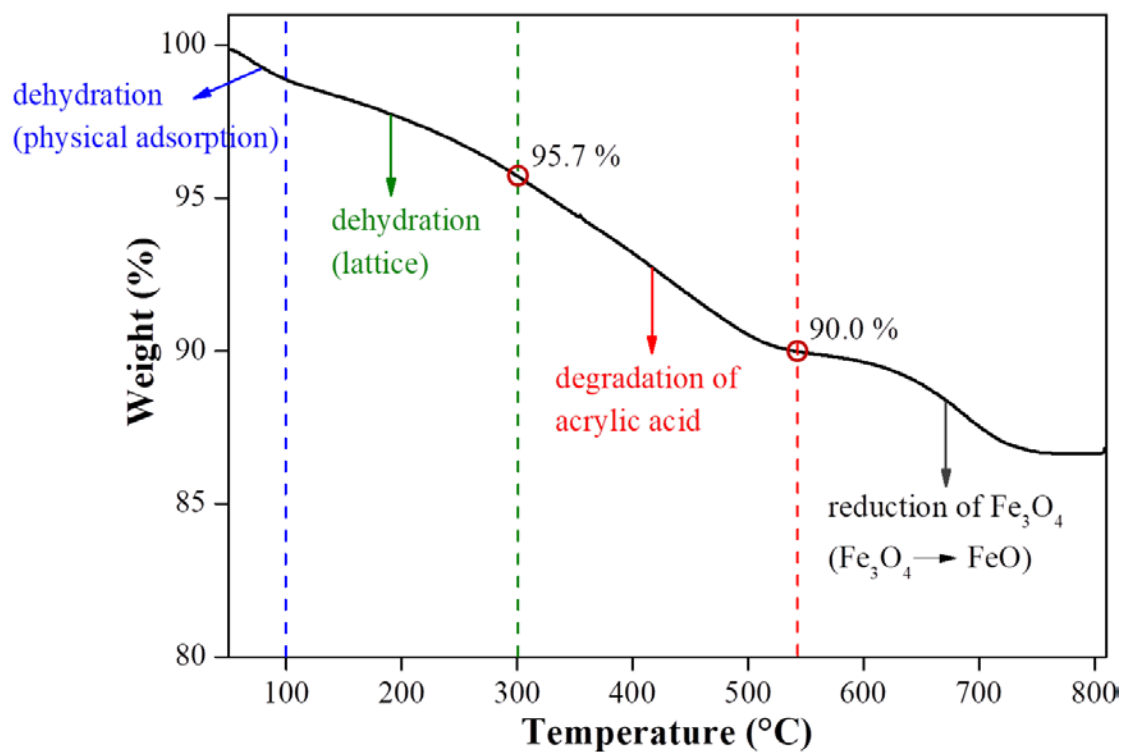


**Figure S2.** TGA curve (conducted in an oxidative environment of air) of the AA-Fe<sub>3</sub>O<sub>4</sub> nanoparticles, in which the weight losses associated with the dehydration (for both the physically adsorbed water and the lattice water), the degradation of acrylic acid, and the reduction of Fe<sub>3</sub>O<sub>4</sub> into FeO were sequentially recorded.<sup>41,42</sup> The weight percentage of the tethered acrylic acid on each AA-Fe<sub>3</sub>O<sub>4</sub> nanoparticle was about 5.96 wt% ( $= \frac{95.7 \text{ wt}\% - 90.0 \text{ wt}\%}{95.7 \text{ wt}\%} \times 100 \text{ wt}\%$ ) and that of the Fe<sub>3</sub>O<sub>4</sub> core was 94.04 wt%.

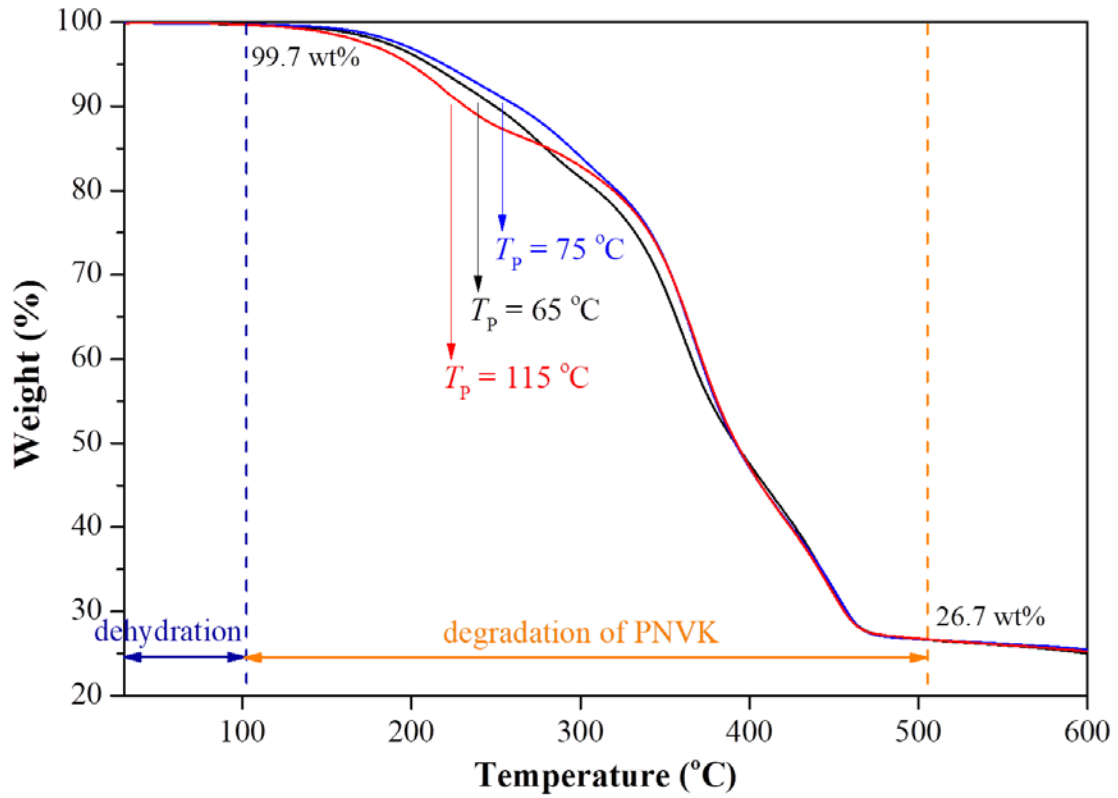


**Figure S3.** TGA curves (conducted in an oxidative environment of air) of the PNVK/AA-Fe<sub>3</sub>O<sub>4</sub>-65 °C, PNVK/AA-Fe<sub>3</sub>O<sub>4</sub>-75 °C, and PNVK/AA-Fe<sub>3</sub>O<sub>4</sub>-115 °C nanocomposites. The weight percentage of the residual Fe<sub>3</sub>O<sub>4</sub> nanoparticles was 26.8

$$\text{wt\%} \left( = \frac{26.7 \text{ wt\%}}{99.7 \text{ wt\%}} \times 100 \text{ wt\%} \right).$$

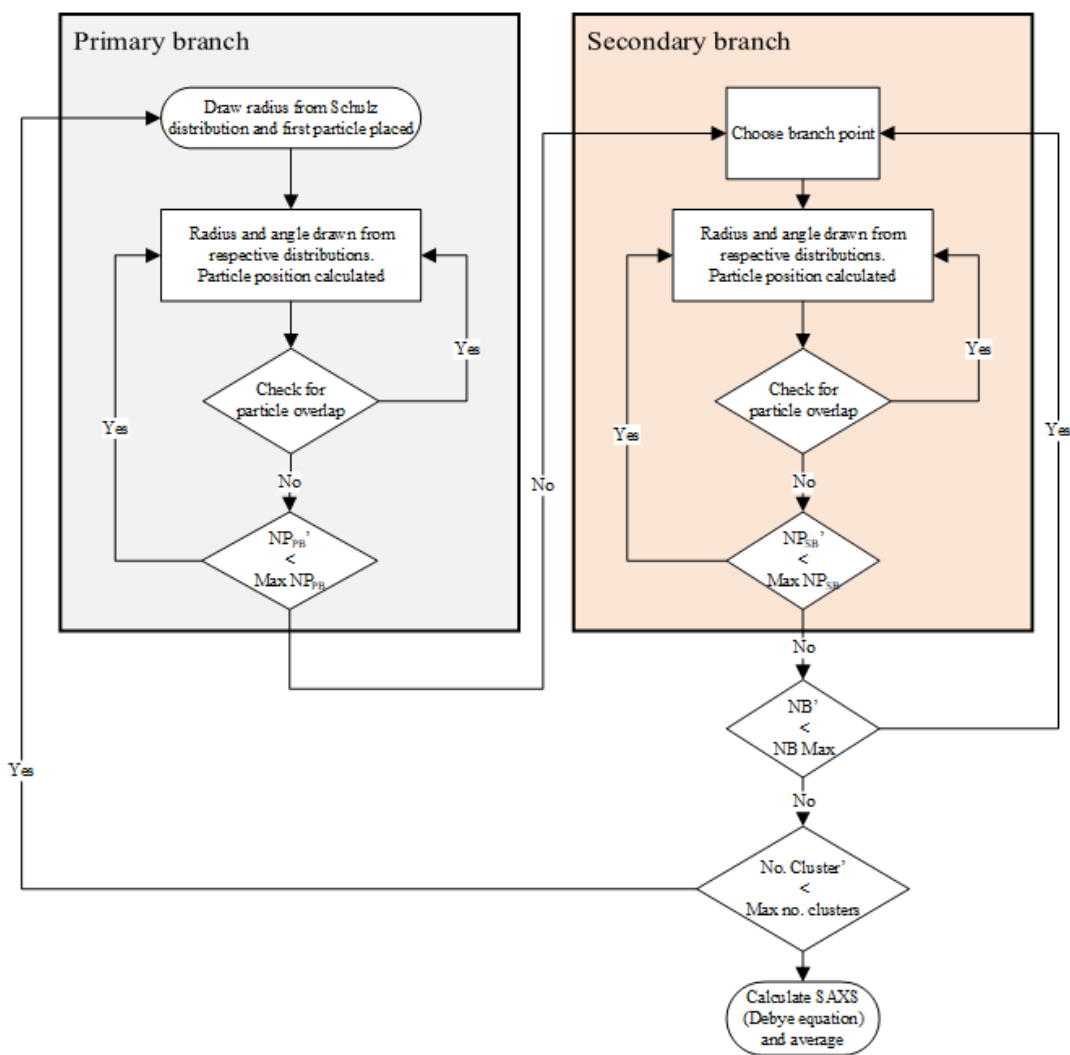


**Figure S4.** Flowchart outlining the code used to build real-space clusters. The left-hand side shows the steps in building the primary branch and the right-hand side shows the steps in building the secondary branches. Particles are placed at the final step of the two branch building sections. The number of particles in the primary branch ( $NP_{PB}'$ ) and in the secondary branches ( $NP_{SB}'$ ) are allowed to reach maximum values (i.e., denoted by  $Max NP_{PB}$  and  $Max NP_{SB}$ , respectively). The number of branches ( $NB'$ ) can reach a maximum value (i.e.,  $NB Max$ ). To achieve good statistics, the maximum number of clusters (i.e.,  $Max no. clusters$ ) controls the total number of

clusters constructed and averaged over.



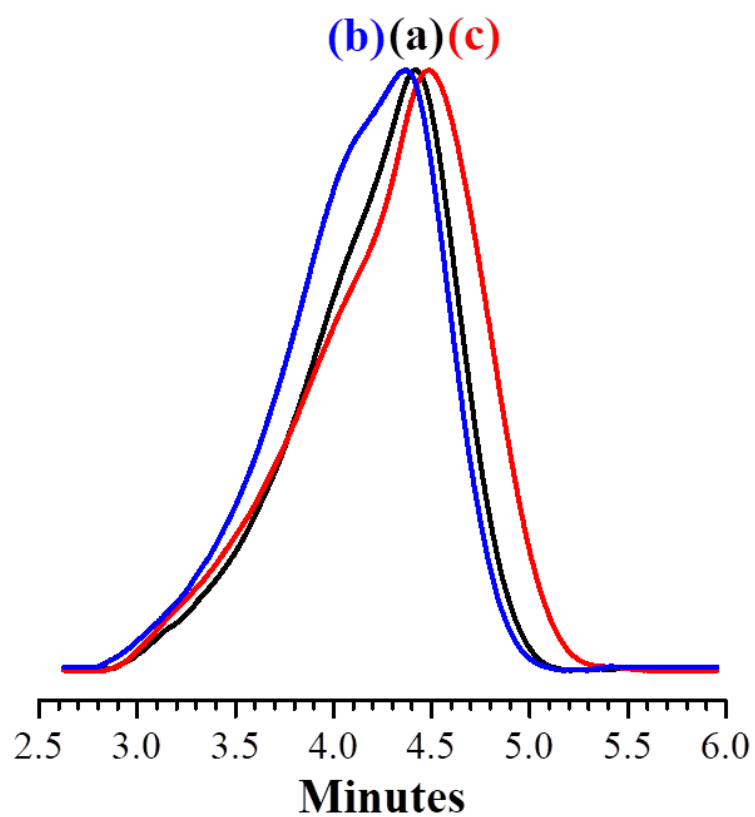


**Figure S5.** GPC curves of the neat PNVK samples prepared via respectively pre-polymerization at (a) 65 °C ( $M_w = 21273$  g/mol,  $M_w/M_n = 2.43$ ), (b) 75 °C ( $M_w = 27882$  g/mol,  $M_w/M_n = 2.94$ ), and (c) 115 °C ( $M_w = 18045$  g/mol,  $M_w/M_n = 2.29$ ) for 3 h followed by polymerization at 100 °C for 3 h (solvent: tetrahydrofuran; temperature: 40 °C).

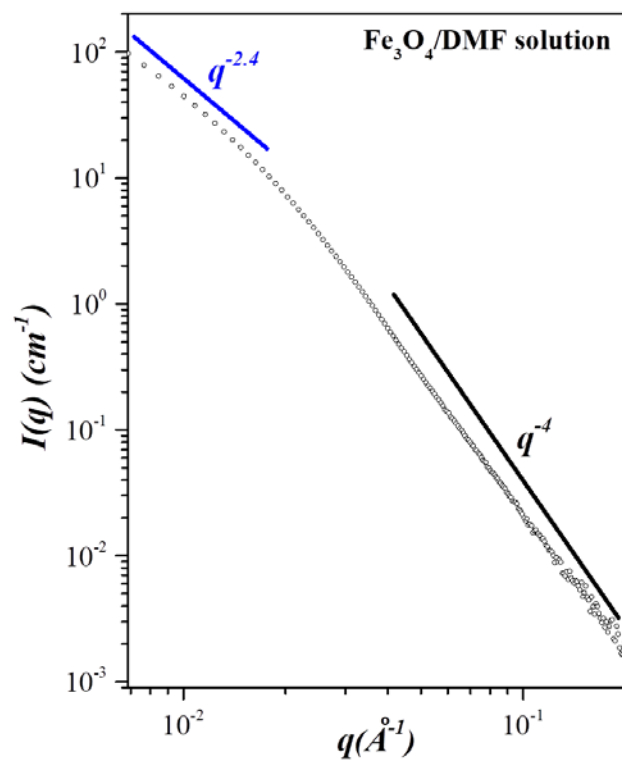


**Figure S6.** SAXS profile of the solution containing Fe<sub>3</sub>O<sub>4</sub> nanoparticles dissolved in the DMF solvent. The volume fraction of Fe<sub>3</sub>O<sub>4</sub> nanoparticles in the solution was 0.0007.

# Neat PNVK

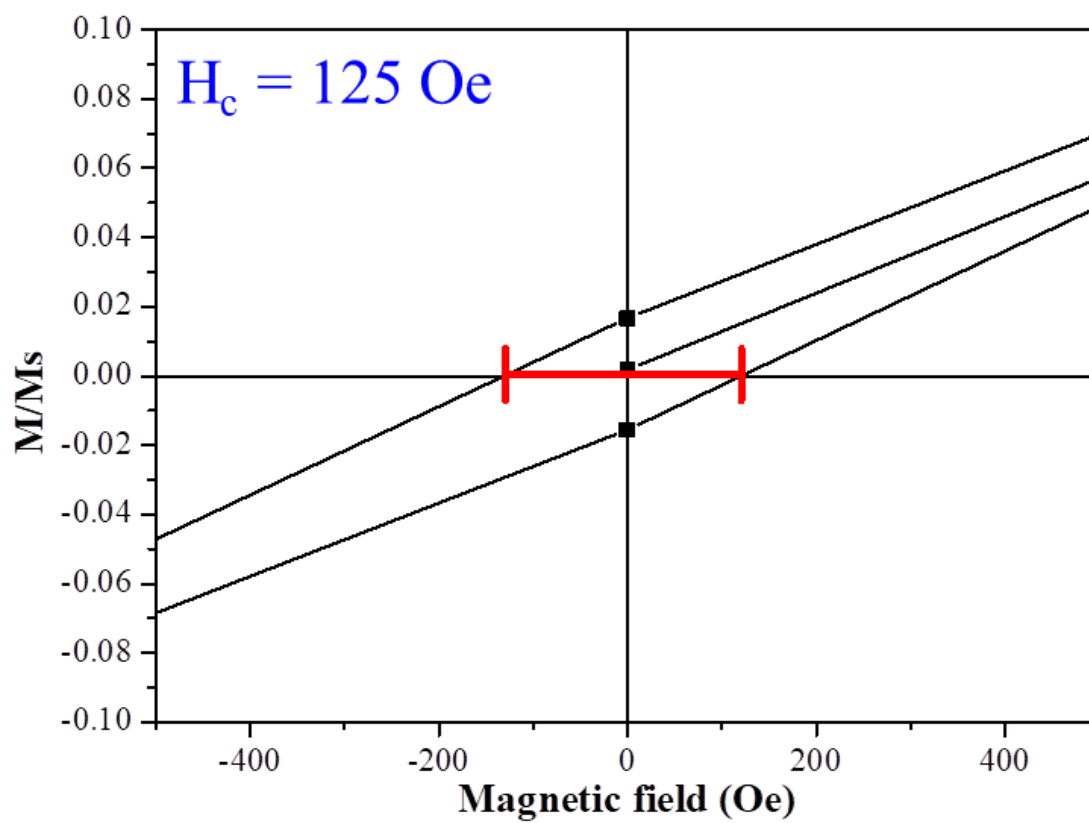


**Figure S7.** Hysteresis loop of the neat PNVK polymer at 300 K.